

Predicting Chronic Pain & Schizophrenia from rs-fMRI data using rDCM

Christian Ohlendorf, James Liu, Saksham Pruthi

30th May 2024

1 Introduction

In our project, we dealt with the question of how an rDCM model can be used on resting state fMRI data in regards to chronic pain. For this, we used the fMRI dataset acquired by Tanaka et al. ([6]). We applied multiple different approaches combining the rDCM model with different classification techniques in order to develop a partition which distinguishes healthy controls from chronic pain patients based on their resting state fMRI. Additionally, we wanted to investigate whether employing sparsity in our model space could also inform our classification and boost the clinical relevance. Particular focus was set on the differences in data-driven and anatomically-informed approaches in regards to their performance as well as interpretability.

Since the results, we achieved with this dataset were very limited, we additionally used the same pipeline on a dataset of schizophrenia patients. This dataset is of a similar size, but achieved a much better classification result. Thus, while our theoretical considerations will be focused on chronic pain, the analysis was mainly done on the schizophrenia dataset.

2 Motivation

Chronic pain is a very multifaceted health condition which can drastically limit the life quality of the person affected. According to ICD-11, it is classified as pain that persists or recurs for more than 3 months ([7]). However, the causes as well as symptoms and disease burden can vary drastically. Yet, there are neuronal mechanisms which are believed to be common to most types of chronic pain.

It is well established that chronic pain reflects in changes in the descending, pain modulation network (DPMN) primarily composed of the periaqueductal gray (PAG), rostral ventromedial medulla (RVM), some other brain stem structures, hypothalamus, amygdala and the dorsolateral prefrontal cortex (dlPFC). Structural and functional changes in this network can result in hyperexpression of pain enhancing signals and reduced inhibition of the ascending pain pathways ([4]). Additionally, the triple network has been found to be altered in chronic pain patients leading to a different subjective experience of pain stimuli. An increased coupling of pain related areas to the default mode network could explain the "chronification" of pain in the sense that pain perturbs perception in the resting state without acute pain stimuli. Additionally, hyperactivity in the salience network has been found to have a modulatory effect on the descending pain pathway. Hyperactivity of the salience network might thus contribute to increased sensitivity to minute pain stimuli. However, it is unclear how exactly the connectivity from the SN to DPMN changes and whether there is enhanced or degenerate connectivity in individuals with chronic pain. It might very well be that the exact SN-DPMN interaction is condition-, or subject specific.

The limbic system might also play an important role since it is involved in emotional processing of pain and thus can also undergo structural changes in chronic pain patients.

Hence, in order to understand the neural mechanisms underlying chronic pain, a large-scale model seems to be necessary. An additional reason for such an approach is that approaches focusing on only one part - see for example ([2]) for an fMRI analysis focusing on the role of the DMN in pain - might allow the distinction of chronic pain patients from healthy controls. However, in other cognitive diseases, like depression or schizophrenia, changes in the DMN are also prime importance [3]). Thus, to our knowledge, there has not been successful attempts to distinguish chronic pain from other conditions based on small-scale networks and whole brain networks might be more promising in this regard.

In addition to subjects diagnosed with chronic pain, we analysed subjects diagnosed with schizophrenia. Initial experiments with chronic pain patients revealed almost no structural differences between healthy controls and chronic pain patients, urging us to check our approach. One of the two possible ways, apart from increasing sample size (which was difficult as the number of chronic pain patients in the dataset were limited), was to check the models and analysis on a separate disorder, for which schizophrenia seemed ideal due to higher sample size and the prevalence of the triple network model in schizophrenia literature.

In regards to the type of model used, models analyzing effective connectivity instead of functional connectivity might give a better insight into the interaction patterns between different brain regions in chronic pain. Dynamic Causal Models can infer on the dependencies of BOLD signals in different regions measured at different points in time, whereas conventional machine learning based typically only capture inter-region dependencies for simultaneous scans (see for example [1]). Since many interactions - especially in large-scale network - occur on the timescale of 100 ms or longer ([8]), these might not be captured by models without this temporal resolution. For these reasons, we chose the rDCM model to estimate effective connectivity from fMRI data and use these parameters as features to a classification model. Our second model class was the sparse rDCM model to check whether introduced sparsity constraints can also provide similar, if not better, performance while reducing model complexity.

3 Modelling Approach

One can generally distinguish between data-driven and anatomy-based approaches to modelling. While the former might achieve better results as it is not based on - possibly inaccurate - assumptions and thus can capture the underlying data structure more closely, it suffers from reduced interpretability. The following table briefly outlines the differences between these two classes:

Table 1: outline of approaches to modelling

	data driven	anatomically informed
BOLD mapping	ICA	parcellation
rDCM	sparse	reduced (Brain Atlas connectome/removal of regions)
analysis	PCA, clustering, classification	inter-region comparisons

3.1 Mapping Scheme

The first design choice is in regards to the mapping of BOLD signals to brain areas. For this, we used the Human Brainnetome Atlas which parcellates the brain into 246 distinct regions. Thus, for each of these brain regions, a BOLD timeseries can be extracted. Using this parcellation scheme has some advantages over other approaches like individual component analysis, since it offers a clearly divided structure based on anatomical considerations - as opposed to ICA, where one has to map the components onto brain structures, thus making overlap between ICs possible. However, we impose a structure on our data which might not necessarily reflect patterns in the underlying neuronal activity in the most accurate way. A further advantage of the Brainnetome Atlas is that it includes a binary connectivity matrix between all regions.

3.2 DCM Model

Since it is unclear, what the best approach to modelling in regards to large-size networks is, we tried multiple different approaches based on rDCM.

3.2.1 Reduced Model

Chronic Pain Based on the considerations of section 3, we constructed a model including only those regions that seem to be relevant for chronic pain. Unfortunately, since the PAG and RVM are not part of the Human Brainnetome Atlas, we could not include these areas and their dynamics directly into our analysis. However, since the subcortical nuclei project to these regions, it might be sufficient to look at higher level regions (subcortical/cortical regions) without considering the actual downstream pain processing pathways.

For determining which areas to include in the reduced model, two heuristics were applied. First of all, we included all areas associated with the triple, limbic and pain networks. We then also looked at the behavioural domains proposed for each region in the Brainnetome atlas. While our chosen areas encapsulated most of the ones here associated with pain, we added one extra region in the inferior frontal gyrus based on this labeling.

The following 131 regions are included in our model:

Schizophrenia For the schizophrenia datasets, we simply used all regions associated with the triple network (104 in total)

Table 2: regions included in the reduced model

region	affiliation	network	Brainnetome regions
SFG	dIPFC	CEN	5,6,11-14
MFG	dIPFC,supplementary motor area	CEN, MN	15-28
IFG	?	pain network?	38
PhG	”	memory	109-120
SPL	SSC2	sensorimotor, DMN	125-134
IPL	gyrus angularis,gyrus supramarginalis	DMN	135-146
precuneus	”	DMN	147-154
PoG	SSC1,M1	sensorimotor	155-162
INS	”	SN	163-174
CG	”	SN, DN, limbic	175-188
Amygdala	”	limbic	211-214
Hippocampus	”	limbic	215-218
basal ganglia	Nac, Pu, Ca, Gp	various	219-230
Thalamus	”	various	231-246

3.2.2 Sparse rDCM

The sparse rDCM was introduced as an addition to the rDCM model. The rDCM model performs quite well for whole-brain effective connectivity and for task-specific fMRI data, however, for some analysis it might become infeasible to use rDCMs. This is primarily due to the large parameter space generated from rDCMs. The sparse rDCMs solve this problem by estimating only a certain fraction of the entire network, which is inferred during its inversion process. This was made possible by adding in a binary indicator variable which works as specifying a Bernoulli distribution given a value of sparsity that you seek from the model. On a higher level, the sparsity acts as an additional prior to make the network architecture informative that a smaller network size might actually be more helpful. The smaller parameter space would be more interpretable and the model complexity lower.

Therefore, for the purpose of our project, in addition to predicting disease conditions, we wanted to test whether a more sparse representation could be informative for the same. This would make it more relevant to a translation to clinical settings due to less number of parameters to interpret and fewer brain regions required to achieve a satisfactory result.

3.3 Classification Approach

We use the connectivity matrix parameter estimates A as generative embeddings for supervised classification. To reduce the amount of redundant connections, we use the Brainnetome Atlas as a mask over the A matrix. We can then flatten the matrix for use as a feature vector for each participant. For sparse variants, we gain an additional z parameter, which represents the posterior probability of connection. To avoid different feature vector lengths across participants, we multiply Az , using z as a weighting. So features from sparse variants are the full 242×242 matrix. Finally to reduce the dimensionality of feature space, we perform Principal Component Analysis, down to dimension $r = 8$. At test time, we project the test data onto the Principal Components obtained on the training data to avoid data leakage.

This formulation is now a standard binary classification setting. We use a Support Vector Machine as the classifier.

4 Datasets

4.1 Chronic Pain

The used dataset is a subset from the aformentioned dataset (imaging site: CIN) and consists of 62 individuals. 24 of these have been classified as suffering from chronic pain. The individuals are of a large age spectrum, from both sexes and of varying handedness. There is no information given on the type or severity of pain or other symptoms like depression. Of these 46 individuals, for 20 healthy controls and 18 patients, timeseries in 242 regions specified by the Brainnetome atlas could be extracted. In all samples, the regions 93, 94, 117, 118 were missing. The first two of those are part of the IFG and therefore are not expected to be of importance. The second two are part of the PhG and thus - as part of the DMN and limbic system - were supposed to be included in the reduced model. Their absence might mean a loss of information, although we do not expect it to be too relevant.

For the other individuals, some further regions were missing which complicates their analysis. For now, we have omitted their analysis after checking that most of the subjects have different regions missing. Thus, the final, balanced set consisted of 18 controls and 18 patients.

Table 3: all used samples for chronic pain (imaging site: CIN)

	subject numbers
patients	1387, 1388, 1389, 1391, 1394, 1395, 1396, 1397, 1398, 1401, 1403, 1405, 1408, 1409, 1410
controls	1364, 1365, 1366, 1368, 1369, 1370, 1371, 1372, 1373, 1374, 1375, 1376, 1377, 1381, 1382, 1383, 1384, 1386

4.2 Schizophrenia

For schizophrenia, we used 2 different sub-datasets also from the set of Tanaka et al. The first one was used in the classification as a training/test set, while the second one was used as an evaluation set. After filtering out the samples without timeseries in all regions and balancing, the final datasets were:

Dataset 1: Imaging site: SWA, 14 controls and 14 schizophrenia patients

Dataset 2: Imaging site: KUT, 17 controls and 17 schizophrenia patients

Table 4: all used samples for schizophrenia (imaging site: SWA)

	subject numbers
patients	0089, 0091, 0094, 0095, 0097, 0098, 0099, 0100, 0102, 0103, 0167, 0191, 0230
controls	0023, 0025, 0026, 0027, 0030, 0031, 0032, 0033, 0034, 0036, 0037, 0038, 0039, 0040

Table 5: all used samples for schizophrenia (imaging site: KUT)

	subject numbers
patients	0670, 0671, 0672, 0674, 0675, 0676, 0678, 0679, 0680, 0681, 0682, 0683, 0684, 0685, 0686, 0687, 0688
controls	0716, 0717, 0718, 0720, 0722, 0723, 0724, 0726, 0727, 0728, 0729, 0731, 0732, 0733, 0734, 0735

5 Methodology

5.1 Pre-processing

The first step was to preprocess the raw fMRI data obtained from the dataset containing information about anatomical aspects (defacing performed) and .nii images for 240 volumes. The entire preprocessing pipeline was performed using the SPM package, and built with small modifications to the preprocessing scripts provided. The 4 major steps were -

5.1.1 fMRI image preprocessing

1. Slice Timing Correction - This step interpolates the slices as if they were captured at the same time, like a temporal alignment of all slices' time series to a specified temporal reference.
2. Motion Correction and Aligning two runs - This step is performed to account for any head movement during the scanning procedure as this might introduce artifacts.
3. Normalisation - The images were normalised using a non-linear transform to a standard template space in order to prevent individual abnormalities and make comparisons standardised.
4. Coregistration - Matching the anatomical data to the functional images using an affine transform to ensure spatial geometries match.
5. Writing Functionals to Standard Space (and Normalisation) - applying above inferred non-linear transform in standard space to promote group analysis.
6. Smoothing - Apply a Gaussian Convolution Kernel to performing blurring to reduce inter-individual differences and increase Signal-to-Noise Ratio.

5.1.2 Generalised Linear Model analysis

The GLM model analysis seeks to model the fMRI signal as a linear combination of given predictors. The basic idea is to input a design matrix of predictors (0s for resting state), perform a convolution with a standard Hemodynamic response function to account for the delay, use a High Pass filter, and perform a model fit using Ordinary Least Squares. We then obtain an activation map and beta coefficients for each predictor.

5.1.3 Extraction of time-series from parcellation (Brainnetome)

We then use the extracted beta estimates to find the BOLD signal change in each voxel, and construct the time-series for each region (averaged over each voxel inside the region) defined using the Brainnetome atlas.

5.1.4 Construction of the DCM

The extracted time-series is then used to construct a Dynamic Causal Model with default settings for each subject using the Tapas package.

5.2 rDCM

For the rDCM inversions without sparsity, we used matlab and the TAPAS package. Inversions were done for a full network of 242 regions as well as a reduced network as described in section 3.2.1. Additionally, we used a model with a threshold on the SNR during inversion in order to see how this affects the results. Since this proved to be non-influential, no analysis was conducted including this threshold.

rDCM inversion were also run in using the Julia implementation of the rDCM package for the same data. This resulted in the knowledge that there is a fundamental difference in the implementations, leading to a difference in the estimates of an order of magnitude.

5.3 sparse rDCM

The sparse rDCM inversions were performed using the Julia rDCM package, kindly provided to us for the purpose of this project. Performing the sparse inversions in Julia were significantly faster than in Matlab. The sparse rDCM was constructed using the DCM generated during the preprocessing and its subsequent conversion into an rDCM to inform sparse rDCM parameters. We tested for 2 values of sparsity only - 0.25 and 0.50 sparsity to inform our model architecture. The inversions were run in parallel on the Euler cluster with one job per subject. The sparse inversion parameters were then stored as in hdf5 file format for use in Matlab and serialized .mat files for use in Julia. We used the connectivity estimates (A matrix) with thresholding using the Posterior for binary indicator variables (z matrix) for further analysis.

5.4 heuristic analysis

We conducted a heuristic analysis of the inter-group differences in the posterior connectivity matrix. Three main components can be extracted from this analysis:

1.

The difference in connectivity strength between two groups averaged over all regions and all samples:

$$D = \frac{1}{N^2} \sum_{i=1}^N \sum_{j=1}^N \frac{1}{K} \left| \sum_{k=1}^K A_{ij}^k - \sum_{k'=1}^K A_{ij}^{k'} \right| \quad (1)$$

where N is #regions, K is #samples per group.

We can calculate this value once for the samples split into the two groups we want to distinguish (i.e. controls and patients) and for random permutations of sample labels which serves as a baseline. The inter-group difference is then:

$$\Delta D = \frac{D_{groups}}{\frac{1}{M} \sum_{l=1}^M D_{perm,l}} \quad (2)$$

where we have averaged over M random permutations. This value gives us an estimate of how large the difference in average connectivity between controls and patients is for the whole network.

2.

A heat map of connectivity differences between controls and patients averaged over samples for each connection. This allows us to analyze which connections are stronger in which group and how important they are.

3.

A 242x242 matrix where only the n largest positive connection differences (i.e. controls on average have a stronger connectivity) and the n largest negative connection differences have a non-zero value. This matrix can be used for visualisation as will be explained later on.

This also allows us to make predictions on group membership based on single connections. To do so, we can take an important connection and rank all samples of a set according to the strength of that specific connection. We then predict the K samples with the largest values to be controls and the other K samples to be patients.

5.5 Model Selection - Free Energy

We have several candidate models as described above. Therefore, we wanted to perform Bayesian Model selection on our candidate selections using the Free Energy derived from rDCM and sparse rDCM inversions among different subject groups.

One caveat with our approach is the fact that the Julia and Matlab implementation of the rDCM is an order of magnitude different, and therefore, the free energy parameter cannot be directly compared.

Nevertheless, the rDCM model with the shortlisted regions for the triple network seemed most promising. However, with the knowledge of difference between Matlab and Julia free energies, we also performed classification using the sparse rDCM models (expected less negative free energy due to lesser features).

5.6 Classification

Feature vectors are obtained using the generative embeddings provided by the rDCM parameter estimates. Even after masking with the Brainnetome Atlas Connectome, the features have dimension $d > 20000$. For a training set of size $n \approx 30$, this would result in overfitting.

For Schizophrenia classification, we have separate training $N_{train} = 25$ and held out test set $N = 34$. This gives us design matrix $X_{train} \in R^{N_{train} \times d}$. Since the number of non-zero principal components is constrained by the rank of the design matrix, we can have a PCA representation of at most N_{train} dimensions. We choose $r = 8$, which explains $\approx 30\%$ of the variance.

5.7 Visualisation

For a visualisation of inter-group connectivity differences, we used the BrainNet module for MatLab [9]. For this, we designed a custom node-set based on the fMRI coordinates of each region specified in the Brainnetome Atlas. The edges were then specified based on the matrix of the n largest inter-group connectivity differences as described in section 5.4. In this context, red edges signify a stronger connectivity in controls and the blue edges a stronger connectivity in schizophrenia patients.

6 results

6.1 Model Selection - Free Energy

The free energy values for the models discussed above clearly show that the rDCM inversions for the reduced models has the least negative free energy among all the other models for subjects across chronic pain and schizophrenia.

Among the Julia models, the 25% sparse rDCM performed marginally better than the 50% sparse rDCM, with both performing better than the rDCM.

However, as described above, it was not possible to directly compare the two free energies from the models inverted in Matlab and Julia. Thus, we decided to keep these models for the next analysis steps.

6.2 chronic pain

Since no meaningful results could be gathered from the chronic pain dataset, we will only present the classification results here and a further analysis in omitted.

reduce_dims	sparse	latent_dim	extra	p0	Train	Cross-Validation	Test
1	0	8	standard	-	0.68	0.60	0.71
1	0	16	standard	-	1.0	0.40	0.43
1	1	8	standard	0.5	0.75	0.6	0.14
1	1	8	standard	0.25	0.68	0.40	0.57
1	1	16	standard	0.5	0.96	0.40	0.43
1	1	16	standard	0.25	0.89	0.60	0.71

Table 6: SVM Classification accuracies for Chronic Pain dataset.

6.3 Schizophrenia

First, we will give a table with all values for ΔD , then a further analysis using heuristics 2 and 3 will follow independently for each model. In these analysis, red/yellow will always signal a stronger connectivity in the control group, while blue signals stronger connectivity in the schizophrenia group.

Table 7: ΔD values for all models and datasets

model	ΔD (dataset 1)	ΔD (dataset 2)
full	1,221	1,094
triple network	1,248	1,109
sparse (50 %)	1,043	1,016
sparse (25%)	1,017	1,003

We consistently get a lower differences between control and patient groups (weighted by random permutations) for dataset 2. We suspect that this is just in the nature of the specific sets due to different test conditions or simply different subjects. Furthermore, the triple network seems to perform slightly better which is to be expected. However, the difference is only marginal, so we conclude that the triple network seems to be only slightly more informative than the whole brain network.

Inducing sparsity reduces the ΔD values drastically. However, we suspect that this is rather an artifact of the differences between the julia and matlab version as mentioned in section 5.5. (This is also supported by the fact that inversion of the full model using julia produced $\Delta D = 1,076$ as opposed to the $\Delta D = 1,221$ achieved by matlab).

6.3.1 full model

heatmaps:

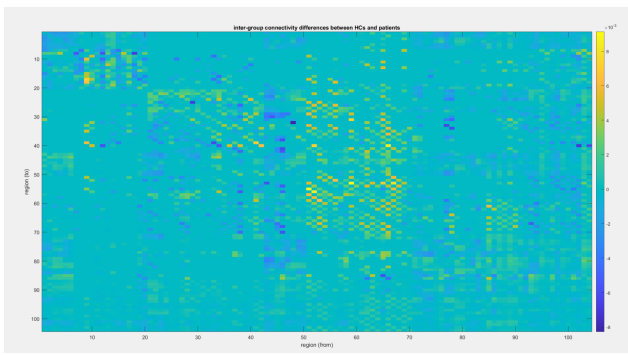


Figure 1: heatmap of connection differences between groups for the full model, dataset 1

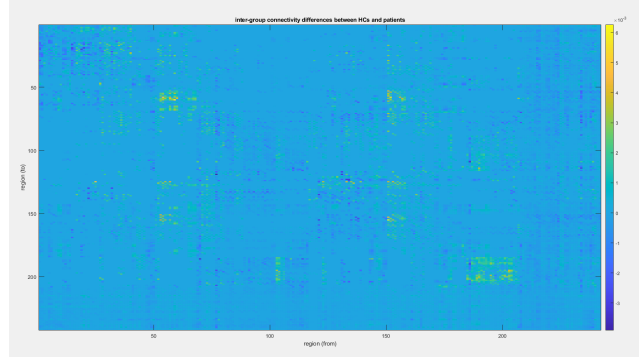


Figure 2: heatmap of connection differences between groups for the full model, dataset 2

The heatmaps are quite similar for both datasets. In particular, we see stronger activity in the controls for columns 50-75 and 150-200 as well as weaker activity for columns 200-242 (which are the subcortical areas). The signal is weaker for dataset 2, as we would expect from the value for ΔD which is also smaller.

Whole brain connectivity visualisation:

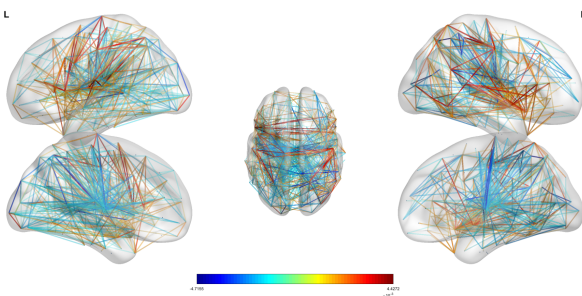


Figure 3: top 1000 connections dataset 1

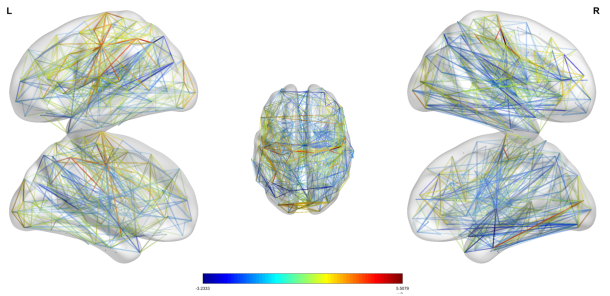


Figure 4: top 1000 connections dataset 2

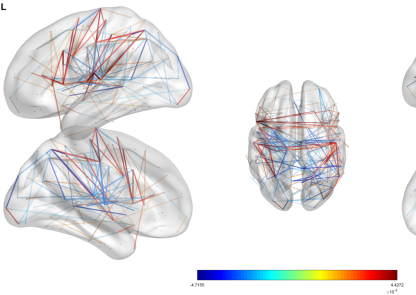


Figure 5: reduced to 30% dataset 1

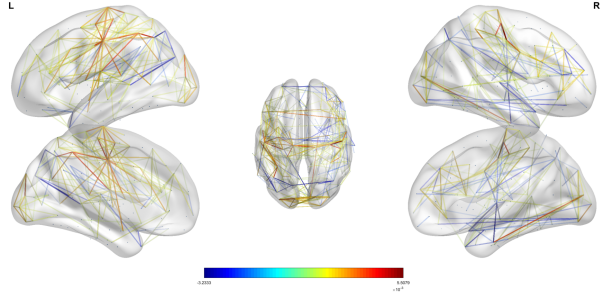


Figure 6: reduced to 30% dataset 2

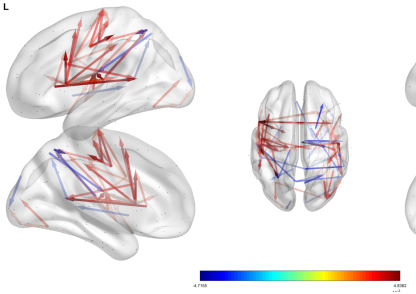


Figure 7: reduced to 7% dataset 1

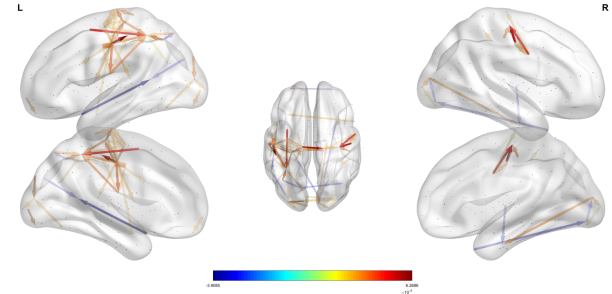


Figure 8: reduced to 7% dataset 2

First of all, we see that in dataset 1 there is more structure as opposed to dataset 2. In the latter, there are some very strong connection differences between subgroups which dominate the rest. This finding also aligns with our values for ΔD , proposing a more extreme distinction between controls and patients for the whole brain in dataset 1. There is no one-to-one mapping in regards to which exact connections are important between the datasets making a comparison quiet difficult. However, there are trends in the connectivity patterns that are applicable to both sets. Since dataset 1 has a stronger, signal, we will focus our further analysis on it.

We can observe strong connectivity going from the ACC and parts of the dlPFC specifically to (sensory)-motor areas, particularly in the left hemisphere. Also, inter-hemisphere connections seem to be primarily within the same level (i.e. between homologous regions). In frontal areas, there is more connectivity in the control group and in parietal/dorsal areas, we can observe a higher activity in schizophrenia patients.

6.3.2 Triple-Network Model

For the triple-network model, we only include the low number of connections visualization since this we generally do not get much new insides. The connectivities look rather similar to before, only that quite some regions are not connected at all as they are not part of the triple network. In the low-connection model, we see similar patterns in the left-hemisphere (although the connections are directed more towards the sensorimotor cortex). In comparison to the full model, we can now see a stronger connectivity in schizophrenia patients from the amygdala and the parahippocampal gyrus to cortical areas like the insula. Surprisingly this is more pronounced in the right hemisphere.

For all other visualisations including the ones on the sparse model, please refer to the presentation.

SVM Results:

reduce_dims	sparse	latent_dim	extra	p0	Train	Cross-Validation	Test
1	0	8	reduce_connect	-	1.0	0.75	0.80
1	0	8	reduce_noise	-	1.0	0.75	0.60
1	0	8	standard	-	1.0	0.5	0.60
1	1	8	standard	0.5	1.0	1.0	0.80
1	1	8	standard	0.25	0.9	0.75	0.80

Table 8: SVM Classification accuracies for Schizophrenic dataset.

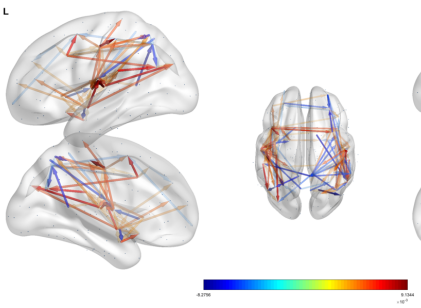


Figure 9: reduced to 7% dataset 1

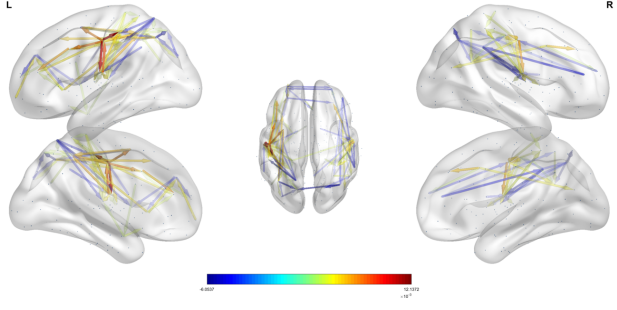


Figure 10: reduced to 7% dataset 2

7 Discussion

For the schizophrenia dataset, we achieved relatively high classification accuracies given the small sample size used which emphasizes the severity of undergoing changes at a whole-brain level. Additionally, we managed to perform meaningful qualitative analyses of the connections that differed most strongly between patients and controls which aligns with known anatomical findings. Specifically, we found stronger connectivity patterns in controls going from the ACC and dlPFC to (sensory)-motor areas. Additionally, using the sparse rDCM, we could find very strong connectivity in sub-cortical areas for schizophrenia patients (not specified in this report, please refer to the presentation for in depth analysis of this point).

7.1 possible shortcomings of chronic pain analysis

Since the single sample rDCM inversions behaved similarly for the chronic pain and the schizophrenia datasets (in regards to free energy, noise precision and power spectral densities), we concluded that issues in the inversion process are probably not responsible for the poor performance of the chronic pain dataset.

The only obvious reason for this result is then that there just is not enough structure in the dataset. For one, this might be due to the limitations already mentioned in section 4. We do not know about the severity and type of pain of the study participants and thus the neural correlate might be too weak to be picked up by the model or confounded by a too diverse group of patients.

Since the schizophrenia dataset has a similar size, we can rule out the sample size as a sole reason. However, it might contribute as a limitation to the already weak signal.

In general, it is expected to have a stronger classification result in schizophrenia as it is a much more severe condition which has an all-encompassing effect on the brain as opposed to chronic pain.

Still, we would have expected a more meaningful result for chronic pain, especially seeing that promising findings have been made using "more primitive" models (see for example [5]).

To see whether the issue laid with the particular dataset or more profoundly in the limitations of our used model for analyzing resting state fMRI of chronic pain patients, a new analysis would have to be made on another chronic pain dataset.

7.2 rDCM and sparse rDCM

The rDCM and sparse rDCM models, especially coupled to the reduced regions, look quite promising to classify disease conditions. It would be interesting to see their estimates compared within different disease models in the future. On the other hand, the sparse rDCM model seems to be tailored around each subject and even though the classification accuracies are comparable, it is yet to be ascertained how exactly to perform inter-subject comparisons apart from focusing on certain regions. Moreover, it also has an optimistic outlook where diagnostics, predictions, and hopefully treatments can be tailored to individual patients.

7.3 Clinical Outlook

The project gives a hint of possibility of incorporating rDCM and sparse rDCM with other traditional diagnostic tools in a clinical setting and thus, directly impact patients suffering from neurological disorders. It would not be a stretch to say that these models can and will have relevance to the medical technology and health industry as a whole.

8 Individual Contributions

The individual contributions can roughly be categorised as follows:

Saksham: preprocessing, (sparse) rDCM inversion in Julia, free energy comparison

Christian: rDCM inversions in matlab, theoretical background on chronic pain, heuristic analysis, visualisation

James: Dense rDCM inversion for chronic pain, dimensionality reduction, classification

However, each of us contributed to all parts of the process by giving helpful input to one another.

We would also like to thank Jerome and Jason for providing us with DCM.mat files for some schizophrenia and control subjects.

References

- [1] Ignacio et al. Cifre. Disrupted functional connectivity of the pain network in fibromyalgia. *Psychosomatic Medicine* 74(1):p 55-62, 2012.
- [2] Peng Liu et al. Partial correlation investigation on the default mode network involved in acupuncture: An fmri study. *Neuroscience Letters*, Volume 462, Issue 3, Pages 183-187, 2009.
- [3] Herman et al. Galioulline. Predicting future depressive episodes from resting-state fmri with generative embedding. *NeuroImage*, Volume 273, 2023.
- [4] M.M Heinricher. Pain modulation and the transition from acute to chronic pain. 2016.
- [5] de Santana Charles Novaes Montoya Pedro Santana Alex Novaes, Cifre Ignacio. Using deep learning and resting-state fmri to classify chronic pain conditions. *Frontiers in Neuroscience*, 13, 2019.
- [6] Yamashita A. Yahata N. et al. Tanaka, S.C. A multi-site, multi-disorder resting-state magnetic resonance image database. *Sci Data* 8, 227, 2021.
- [7] Rolf-Detlef et al. Treede. A classification of chronic pain for icd-11. 2015.
- [8] Martin Vinck, Cem Uran, Georgios Spyropoulos, Irene Onorato, Ana Clara Broggini, Marius Schneider, and Andres Canales-Johnson. Principles of large-scale neural interactions. *Neuron*, 111(7):987–1002, 2023.
- [9] He Y Xia M, Wang J. Brainnet viewer: A network visualization tool for human brain connectomics, 2013.